Flight-induced compass representation in the monarch butterfly heading network

M. Jerome Beetz [1]*, Christian Kraus[1], Myriam Franzke[1], David Dreyer[2], Martin F. Strube-Bloss[3], Wolfgang Rössler[1], Eric J. Warrant[2], Christine Merlin[4], Basil el Jundi[1]*

Affiliations

[1]Zoology II, Biocenter, University of Würzburg, Würzburg, Germany

[2]Lund Vision Group, Department of Biology, Lund University, Lund, Sweden

[3]Department of Biological Cybernetics, University of Bielefeld, Bielefeld, Germany

[4]Department of Biology and Center for Biological Clocks Research, Texas A&M, College Station, TX, USA

*Corresponding authors

Email:

M. Jerome Beetz: jerome.beetz@uni-wuerzburg.de

Basil el Jundi: basil.el-jundi@uni-wuerzburg.de

Keywords: navigation, orientation, migration, central complex, sun compass

Short title: State-dependent compass coding

Abstract

For navigation, animals use a robust internal compass. Compass navigation is especially crucial for long-distance migrating animals like monarch butterflies, which use a sun compass to navigate every fall over 4,000 km to their overwintering sites. The central complex, a brain region equipped with sun-compass neurons, is proposed to control the butterfly's heading. Although the activity of central-complex neurons exhibits a locomotor-dependent modulation in many insects, the consequences of such modulations for the coding of heading remain unexplored. Here, we developed tetrode recordings from tethered flying monarch butterflies to reveal how flight modulates heading representation. We found that during flight, heading-direction neurons change their tuning, transforming the central-complex network to function as a global compass. This compass coding is characterized by the dominance of steering feedback and allows for robust heading representation even under unreliable visual scenarios, an ideal strategy for maintaining a migratory heading over enormous distances.

Introduction

Goal-directed navigation requires animals to constantly register their heading in space. This is of particular importance during long-distance migration, as exhibited by many vertebrates, such as birds and bats [1]. Similarly, monarch butterflies (*Danaus plexippus*) annually migrate from southern Canada and the northern United States to their overwintering habitat in central Mexico [2,3]. To maintain proper migratory direction, monarch butterflies rely on an internal compass that integrates multimodal orientation signals, including the sun [4,5]. Sun compass information is processed in a brain region termed the central complex [6,7]. In this brain region, compass neurons are thought to encode the butterflies' heading, like head-direction cells in vertebrates [8-12]. Data from the central complex of *Drosophila* show that heading is topographically represented in a neural network composed of E-PG cells [13-15]. Within the E-PG network, heading is represented by a single activity bump that changes its position when the insect changes its heading direction [13,16]. The activity bump in E-PG cells results from the integration of visual signals and mechanosensory information [14,17-19], as well as idiothetic, self-motion signals [13,20,21]. Although the multimodal input may explain locomotor-dependent modulations in the activity of central-complex neurons [22,23], the function of these state-dependent modulations is still poorly understood. To shed light on this, we investigated how the locomotory state affects sun compass coding in the monarch butterfly.

In the past, due to methodological limitations, butterfly' sun compass neurons have only been recorded in restrained animals [6]. Here, using monarch butterflies, we investigated how the heading-direction network operates when the animal is free to steer with respect to a sun stimulus. We observed that when the animals were free to steer during flight, the heading-direction network modified its angular tuning, i.e. remapped from a vision-based sun-bearing coding found in quiescent animals to a compass coding during flight. The transformation to a compass was reflected by a state-dependent change in angular sensitivity and tuning. At flight onset, a substantial number of neurons started to encode the solar azimuth, while others ceased to encode the sun position, a process that depends on changes in octopamine levels. Changes in angular tuning were accompanied by a state-dependent switch in cue hierarchy between visual and idiothetic inputs. Importantly, the heading-direction network transformed into a compass that was dominated by idiothetic cues when the tethered flying butterflies were allowed

to perform actual turns. The dominance of idiothetic cues allowed a robust heading representation even under ambiguous or conflicting visual settings. Thus, in the monarch butterfly central complex, flight activity shapes the heading-direction network into a multimodal, global compass that allows these insects to reliably maintain their migratory southward direction.

Results

State-dependent changes in angular sensitivity of central-complex neurons

To perform tetrode recordings from tethered flying butterflies, we designed an indoor flight arena (Fig. 1A). The arena's upper inner circumference was equipped with a strip of individually switchable green light spots serving as sun stimuli that butterflies could use for orientation. During neural recordings from the central complex of tethered butterflies centered in the arena (Fig. 1B, Supplementary Figure 1), an optical encoder measured the animal's heading direction. First, we recorded from quiescent butterflies that rested on a platform at a fixed heading (0°; *quiescent pre-flight*; Supplementary Movie 1) and that were stimulated by moving the sun stimulus along a 360° circular path around the animal. To investigate the influence of proprioceptive effects from flight activity on the neural response, we then presented the same sun stimulus, but now with the butterfly flying at a fixed heading (0°; *fixed flight*; Supplementary Movie 2). A subset of central-complex neurons (66 of 150 recorded neurons; 44%) exhibited state-dependent angular tuning to the sun stimulus. During *fixed flight*, 50 neurons (33%; 8 + 29 + 13 neurons outside the gray area in Fig. 1C) encoded the solar azimuth as indicated by an increase in firing rate at neuron-specific azimuthal positions of the sun stimulus (Rayleigh test: $p < 0.05$). In contrast, during quiescence, the same neurons showed stable firing rates across different sun positions (Rayleigh test: $p > 0.05$) and therefore did not encode the solar azimuth (Fig. 1D, green dataset). Conversely, 16 neurons (11%, 2+14 neurons of gray area in Fig. 1C) showed angular sensitivity during quiescence but ceased to encode the solar azimuth during *fixed flight* (Fig. 1D, blue dataset). The remaining 84 of the 150 recorded neurons (56%) did not change their angular sensitivity to the sun stimulus during fixed flight: 76 neurons were sensitive (51%; 56 + 20 neurons in merged gray and blue areas of Fig. 1C) and 8 neurons insensitive (5%; green area in Fig. 1C) during both locomotory states. To test whether changes in angular sensitivity reflect recording instability, e.g.

subtle electrode movements induced by flight, we allowed the butterfly to settle on the platform after flight and retested the neural sensitivity in 63 neurons (*quiescent post-flight*). All 63 neurons retained their *quiescent pre-flight* angular sensitivity (example shown in Fig. 1D), suggesting that changes in angular sensitivity observed during flight depended solely on the animal's locomotory state. We also excluded that we recorded from different neurons across the behavioral states by assessing the spike-shape stability. This was done by computing the averaged spike shapes from each neuron and locomotory state (i.e., *quiescent pre-flight*, *fixed flight*, and *quiescent post-flight*). These averaged spike shapes were correlated with each other, and the correlation coefficients were statistically compared with the ones obtained by correlating neuron-specific spike shapes with averaged spike shapes of randomly chosen neurons (Fig. 1E-1F, cf. Online Methods). For all neurons of the present study, the averaged spike shapes within spike-sorted neurons statistically correlated better than with averaged spike shapes across different neurons. This strongly suggests that we recorded from the same neurons throughout the entire experiment.

Next, we examined how state-dependent changes in angular sensitivity are reflected in the broadness of neural tuning. For each neuron and locomotory state, we calculated the neuron's vector strength. The higher the vector strength, the narrower the neural tuning, and vice versa. As expected, neurons that started to encode the solar azimuth during fixed flight (Rayleigh-test: $p < 0.05$) exhibited higher vector strengths during *fixed flight* compared to *quiescence* (Wilcoxon signed rank test: $p < 0.0001$; green data points in Fig. 1G-1H). In contrast, neurons that ceased to encode the solar azimuth during *fixed flight* (Rayleigh test: $p > 0.05$) had lower vector strengths during *fixed flight* compared to *quiescence* (Wilcoxon signed rank test: $p < 0.0001$; blue data points in Fig. 1G-1H). Neurons encoding the solar azimuth irrespective of the animal's locomotory state showed broader tuning during *fixed flight* compared to *quiescence* (Wilcoxon signed rank test: $p < 0.0001$; orange data points in Fig. 1G-H).

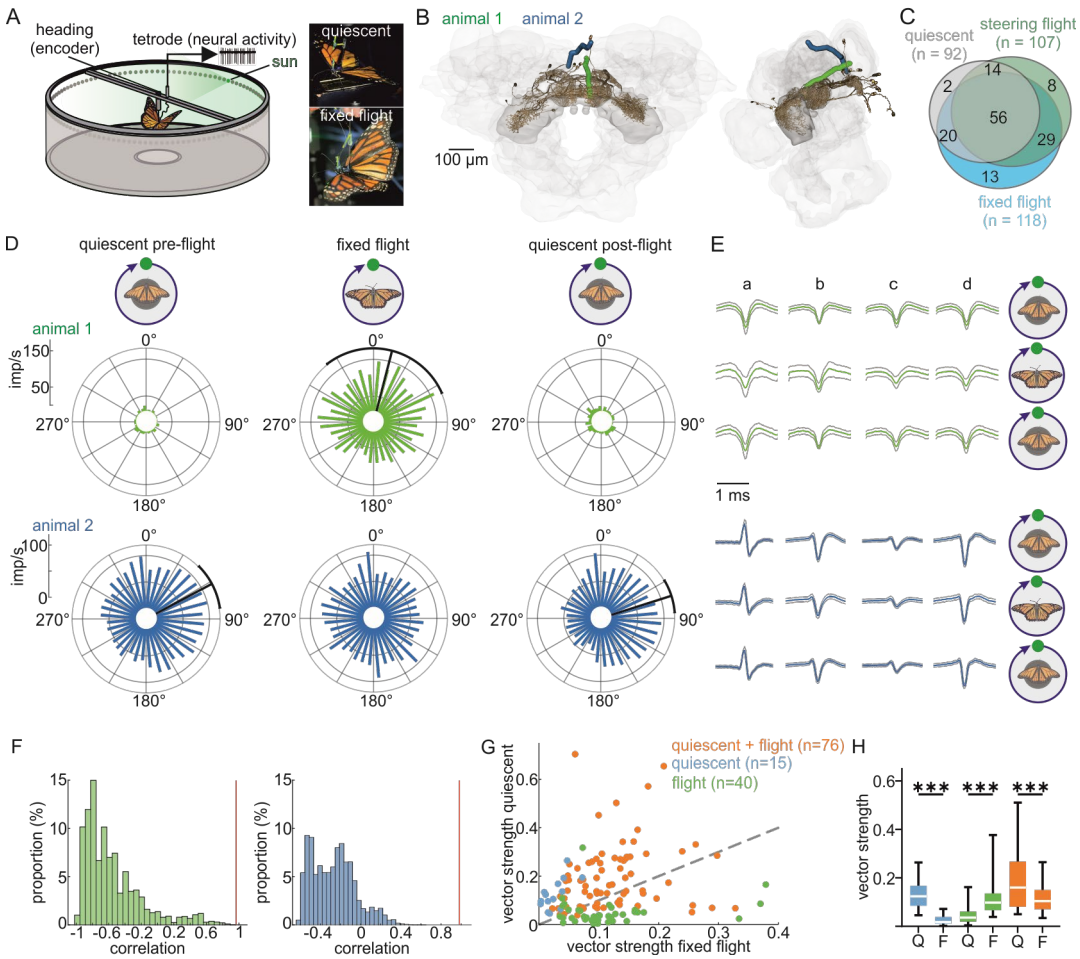

Fig. 1 | State-dependent change in angular sensitivity in butterfly central-complex neurons. A, Schematic drawing of the setup. **B**, Anterodorsal (*left*) and lateral (*right*) view of reconstructed tetrode tracks from two animals (*blue and green*) warped into the standardized monarch butterfly central complex [7] including prominent central-complex neurons [7] (*brown*). **C**, Number of neurons showing angular sensitivity to the sun stimulus across different behavioral states, i.e. *quiescent, fixed flight, steering flight*. **D**, Responses of two example neurons (*blue*, *green,* same color code as in B) to the moving sun stimulus (animals faced 0°) in different behavioral states, i.e. *quiescent pre-flight (left), fixed flight (middle), quiescent post-flight (right)*. *Black line* and *arc* represent the preferred firing direction ± circular SD of neurons that encoded the solar azimuth (Rayleigh test: $p < 0.05$). **E**, Spike shapes (*mean ± IQR*) of individual tetrode channels (*a-d*) for each behavioral state for the *blue* and *green* neurons shown in (D). **F,** Comparison of the spike shape correlation (for the *blue* and *green* neuron in D) between two behavioral states (*red vertical line*) and a modelled distribution of spike correlations. **G,** Comparison of vector strengths calculated for *quiescent* and *fixed flight*. Neurons that showed angular sensitivity exclusively during *fixed flight* and *quiescence* are shown in *green* and *blue*, respectively. Neurons encoding the solar azimuth in all locomotion states are indicated in *orange*. **H**, Statistical comparison of vector strengths across locomotion states (Q = *quiescent*; F = *fixed flight*; Wilcoxon signed rank test: *** = $p < 0.001$).

131 **Remapping of the heading-direction network during steering flight**

132 To test if changes in heading coding occurred when tethered flying butterflies were free to rotate
133 around their yaw axis while the sun stimulus was set at 0° (*steering flight*; Supplementary Movie 3). We
134 classified 70 of the 150 recorded neurons as encoding the solar azimuth during *quiescence* and *steering*
135 *flight* (Fig. 2A-C; 47% of the neurons; 14 + 56 neurons of gray portion in Fig. 1C). While some neurons
136 showed a similar angular tuning across *quiescence*, *fixed*, and *steering flight* (magenta neuron in Fig.
137 2A-C), many others shifted their preferred firing direction, during *steering flight* compared to *quiescence*
138 (Fig. 2C, black lines in circular plots of blue neuron; Supplementary Figure 2), suggesting a remapping
139 of the neural network. When comparing the neural response across a population of 27 neurons that were
140 sensitive at each behavioral state, we found that the remapping mainly occurred during *steering flight*
141 (Fig. 2D) but rarely between *quiescence* and *fixed flight*, and *quiescence pre-* and *post-flight* (Fig. 2E
142 and 2G; respectively, n = 76 and 46 for *quiescent* versus *fixed flight* and *quiescent pre-* versus *quiescent*
143 *post-flight*; V-test: $p < 0.0001$). The shifts in angular tuning during *steering flight* were arbitrary across
144 neurons, indicated by a uniform distribution (Fig. 2F; Rayleigh test: $p = 0.09$, n = 70). While, during
145 flight, the relative angular position between butterfly and sun stimulus dynamically changed with the
146 butterfly' heading direction, stimulus history and velocity were constant in quiescence. To exclude the
147 possibility that the observed remapping resulted from differences in the spatiotemporal dynamics of the
148 stimulus, we measured the neural tuning when the sun stimulus unpredictably moved at different
149 directions and velocities in quiescence (Supplementary Movies 4 and 5; Supplementary Figure 3A-C; n
150 = 42 neurons). We found that the neural tuning was neither affected by stimulus history nor stimulus
151 velocity (V-tests: $p < 0.001$). Remapping could also be evoked by the coding of turns [20,21,24], which may
152 obscure angular tuning to our sun stimulus. Only 7 (5%) of our 150 recorded neurons conjunctively
153 encoded flight turns and heading (example neuron in Supplementary Figure 3D-E), confirming that
154 coding of angular turns was not responsible for remapping. Taken together, our data suggest that the
155 remapping in the heading-direction network mainly occurs during *steering flight* and is dependent on
156 the animal's locomotory state.

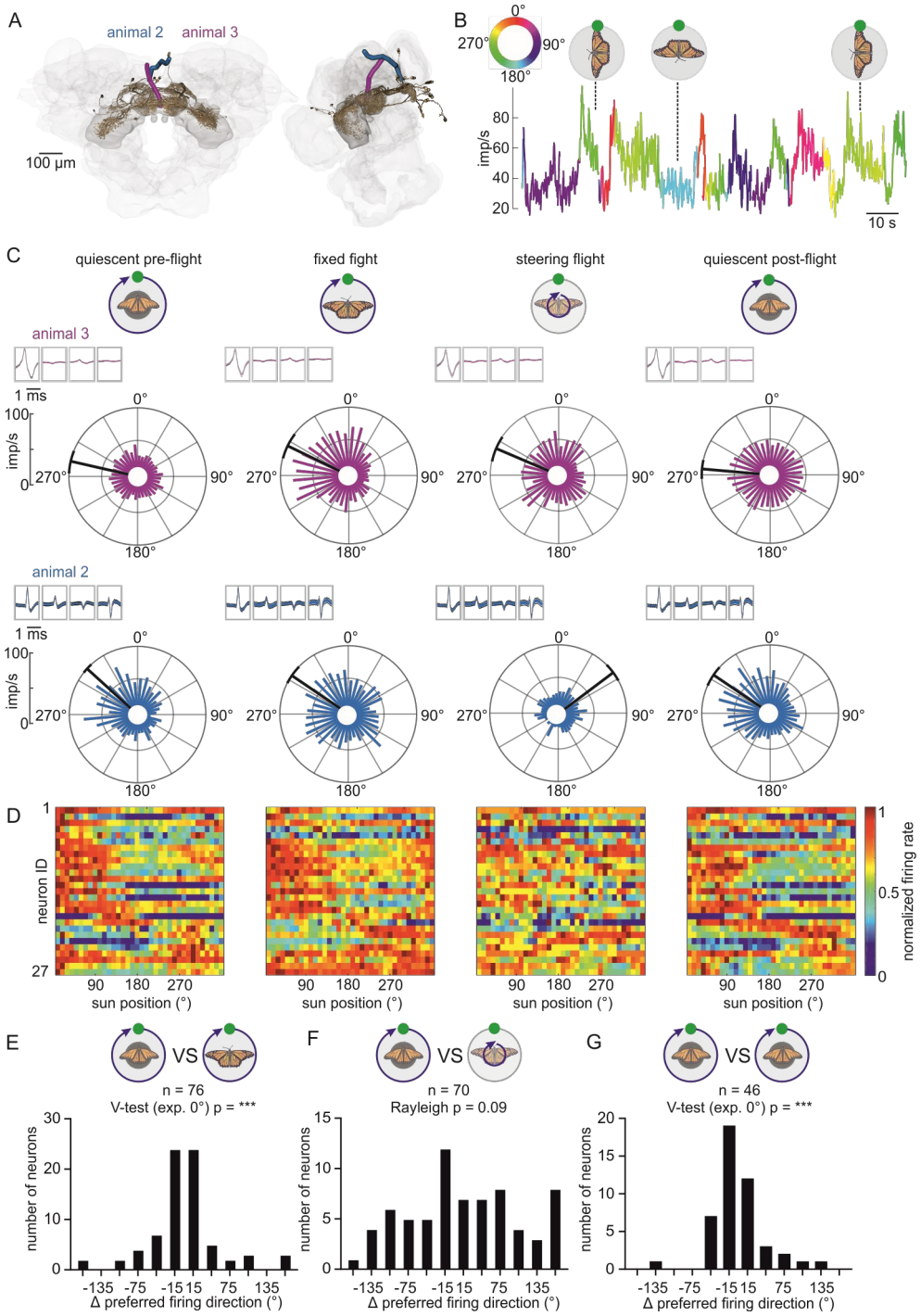

Fig. 2 | State-dependent changes in angular tuning of butterfly central-complex neurons. A, Reconstructed tetrode tracks one from each animal, indicated in different colors. **B**, Neural firing rate from a central-complex neuron as a function of the animal's heading coded in color. The neuron increased its firing rate when the animal was heading at 270° while neural activity decreased when the animal was heading at 180°. **C,** Firing rates of two neurons (*magenta*, *blue*) at different sun positions relative to the animal's heading (pointing towards 0°) for four behavioral states. Corresponding spike shapes (*mean* ± *IQR*) are indicated at the top left corner of each circular plot. **D,** Neural activity (color coded) of 27 neurons (*y-axis*) plotted against the sun position (*x-axis*) for each behavioral state. Only neurons that were sensitive (Rayleigh test: $p < 0.05$) across all four behavioral states are included. For all neurons that were sensitive during *quiescence* and *steering flight* see Fig. S3. **E-G**, Changes in preferred firing direction between *quiescent pre-flight* and *fixed flight* (E), *quiescent pre-flight* and *steering flight* (F), and *quiescent pre-flight* and *quiescent post-flight* (G).

A 360° compass of heading angles is computed during flight

While in *Drosophila*, remapping of the heading-direction network could be induced by presenting different visual scenes [14,15], a state-dependent remapping was not found [14]. In contrast to this, we here demonstrate for the first time a state-dependent remapping in the heading-direction network of a long-distance migrating insect. To understand the biological role of state-dependent remapping in monarch butterflies, we compared the distribution of preferred firing directions during *quiescence* with the distribution during *steering flight*. During *quiescence*, the neurons predominantly encoded the butterfly's frontal hemisphere ($n_{quiescent} = 92$ neurons; Fig. 3A; V-test: $p < 0.001$), while during *steering flight* the neurons fully tiled 360° representation of heading ($n = 107$; Fig. 3B; Rayleigh test: $p = 0.83$). These results strongly suggested that the heading-direction network changes its coding strategy and only functions as a compass when the butterfly is flying.

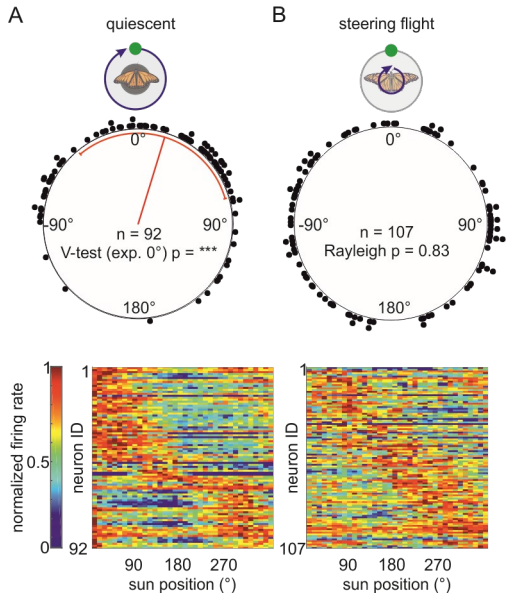

Fig. 3 | State-dependent transition of the butterfly central complex to a compass. upper A-B, Distribution of the preferred firing directions during *quiescence* (A) and *steering flight* (B). The preferred firing directions were biased towards the frontal visual field during *quiescence* while they showed a uniform 360° distribution during *steering flight*. **lower A-B**, Neural activity (color coded) of respectively 92 neurons and 107 neurons plotted against the sun position (*x-axis*) for quiescence (*left heatmap*) and steering flight (*right heatmap*). Differences in the number of neurons in each colormap come from the fact that only neurons that were sensitive (Rayleigh test: $p < 0.05$) to the respective locomotion-state were considered.

To characterize the coding strategy of the heading-direction network across different locomotory states flight, we performed experiments where we tested the neural coding of the same neurons in quiescent and flying butterflies but from butterflies presented with an ambiguous visual stimulus i.e., two suns set 180° apart (2-sun experiment). When the two suns were rotated by 360°

around a quiescent butterfly (Fig. 4A; *quiescent pre-flight* in Fig. 4B-C), heading-direction neurons showed a bimodal response reflecting the 180° periodicity of the visual stimulus. This bimodal response was consistent across each full stimulus rotation (middle column in Fig. 4B) indicating that the heading-direction network of quiescent butterflies equally weighted and computed both suns as isolated visual cues. In contrast, the same neurons represent the visual scene by a unimodal response during steering flight (Fig. 4A; *steering flight* in Fig. 4B-C). Thus, the network forms a compass that globally integrates both suns into a 360° visual scene and allows the butterfly to encode an explicit heading. Importantly, as soon as the animal settled (*quiescent post-flight*), the heading-direction network only receives visual information and therefore exhibited a 180° periodicity in heading coding, similar to the coding observed prior to flight (Fig. 4B-C). State-dependent transitions between unimodal and bimodal responses were highly significant (Fig. 4D; RM one-way ANOVA + Holm Sidák's multiple comparison test: $p < 0.001$, $n = 33$ neurons). Together, these results demonstrate a state-dependent functional remapping in the central complex: In quiescence, the heading-direction neurons represent heading in a visual-based sun bearing coding. In contrast, the same neurons transform into a compass coding during flight, which allows butterflies to maintain all possible heading directions in a body invariant manner.

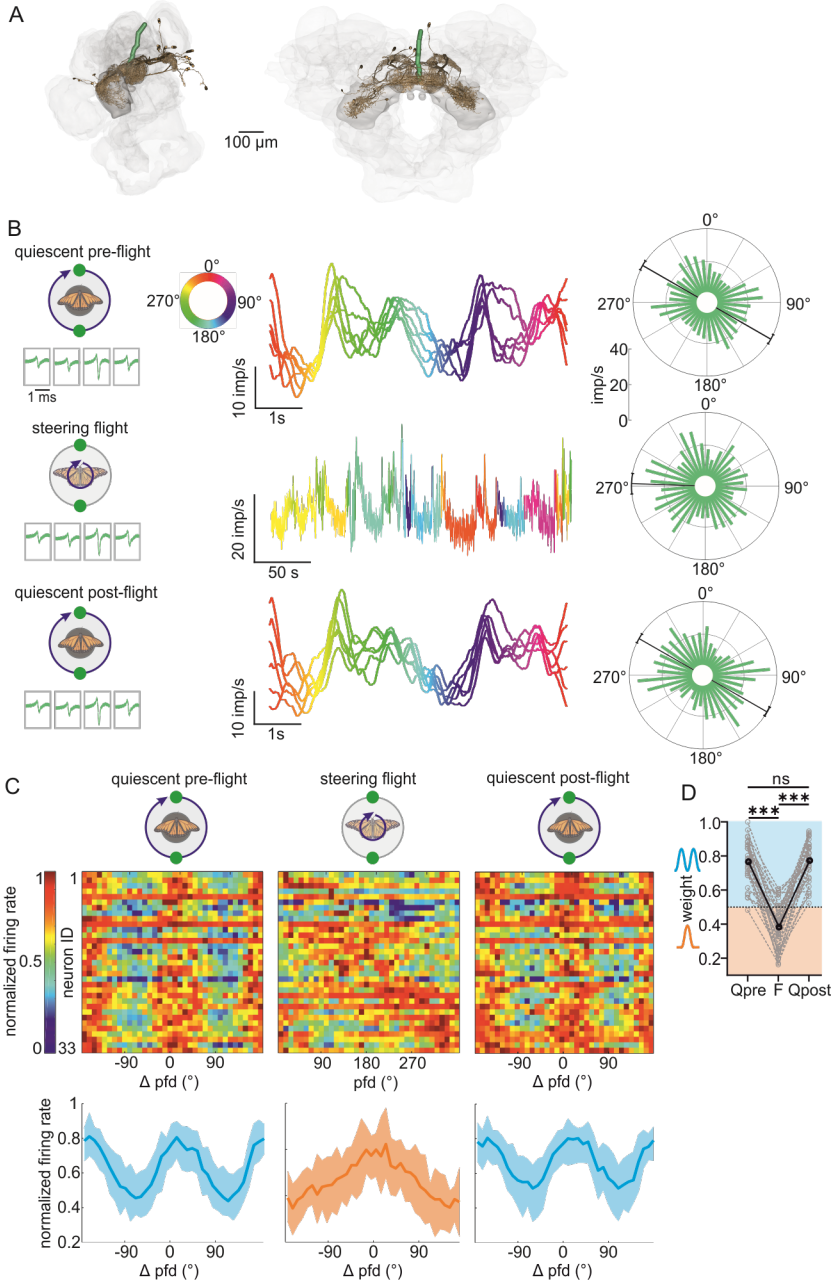

Fig. 4 | Heading coding of central-complex neurons under an ambiguous visual scene. **A**, Tetrode position of the neuron recorded in (B). **B**, The neural response to the 2-sun stimulus in quiescent (stimulus was rotated 6 times around the animal; *first and third row*) and flying monarch butterflies (static stimulus; *second row*). (*Left*) Average spike shapes are shown below the schematic icons. (*Middle column*) Neural response to individual stimulus rotations (sun azimuth is color coded) in *quiescence* and the response of the same neuron during flight (animal's heading color coded). (*Right*) Circular plots summarize the neural tuning for the respective locomotion state. **C**, (*Top*) Responses of 33 neurons in each behavioral state. Along the x-axis, the heatmaps are centrally aligned to the neuron's preferred firing direction (*pfd*) in the *quiescent pre-flight* condition. Along the y-axis, the neurons are ordered according to the pfd measured during steering flight. (*Bottom*) Averaged response (mean ± quantile) of all 33 neurons during quiescence (*left*, *right*) and during flight (when the neurons' maximum responses were shifted to 0°). **D**, Weights of the responses of the 33 neurons to a bimodal or unimodal model for each behavioral state, i.e. *quiescent pre-flight* (Q_{pre}), *steering flight (F), quiescent post-flight* (Q_{post}). A weight between 0 and 0.5 indicates that the neural response was unimodal, whereas a weight between 0.5 and 1 indicates that the neural response was bimodal. Mean weights are indicated by black lines. Friedman test: *** = $p < 0.0001$; ns = $p > 0.05$.

225 **Octopamine changes angular sensitivity**

226 What mechanisms underly the state-dependent transformation into a sun compass during flight?
227 As some neurons increased their firing rates during flight (e.g., Fig. 1D, green neuron), we wondered
228 whether changes in neural firing rate contribute to the state-dependent changes in angular sensitivity.
229 We found that this was not the case as changes in neural firing rates during quiescence (pre- & post-
230 flight) and flight (Fig. 5A) were not sufficient to induce any state-dependence changes (orange data
231 points in Fig. 5A). In flies, the neuromodulator octopamine, the invertebrate analog of noradrenaline [25],
232 is expressed during flight and has been linked to state-dependent changes in the neural sensitivity of
233 optic lobe and descending neurons [26,27]. To test if octopamine could mediate the state-dependent changes
234 we observed in the heading-neural network, we topically applied chlordimeform (CDM), an octopamine
235 agonist, onto the brain of quiescent butterflies (N = 13 animals; n = 50 neurons) to mimic potential
236 flight-induced physiological effects [26,28]. Following CDM application, eight neurons (15 %, Fig. 5B-C,
237 cyan neuron; neuron ID 17-24 in Fig. 5D) started to encode the solar azimuth, whereas 16 neurons (31
238 %, Fig. 5B-C, magenta neuron: neuron ID 1-16 in Fig. 5D) lost angular sensitivity. For the remaining
239 26 neurons (51 %), we could not detect an effect of CDM on angular sensitivity. The vector strength of
240 neurons from CDM-treated *quiescent* butterflies was similar to that for neurons of non-treated butterflies
241 during *fixed flight* (compare magenta /cyan data points in Fig. 5E-F and blue/green data points in Fig.
242 1G-1H). While flight-induced changes in angular sensitivity could be mimicked by CDM treatment,
243 CDM did not however induce any remapping (Fig. 5G, V-test: $p < 0.001$). These results suggest that
244 idiothetic cues exclusively processed during steering flight are responsible for remapping the butterflies'
245 heading-direction network into a sun compass.

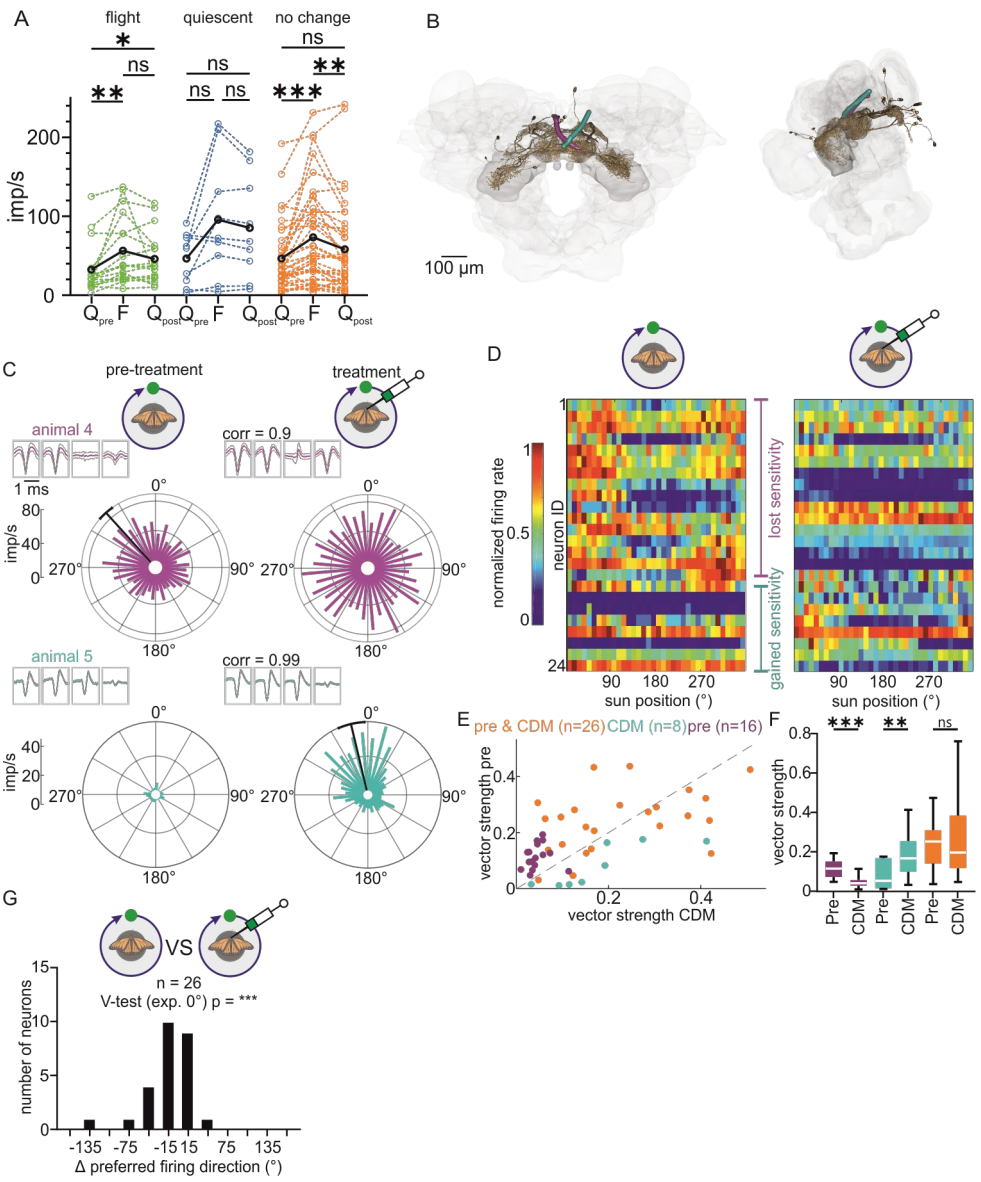

Fig. 5 | Changes in angular sensitivity after chlordimeform (CDM) application. A, Mean firing rates at different locomotion states, i.e. *quiescence* (pre: Q_{pre} and post: Q_{post}) and *fixed flight* (F) for three different neuron subpopulations. *Green neurons* (n = 50) were sensitive only during *fixed flights* while *blue neurons* (n = 16) were sensitive only during *quiescence*. *Orange neurons* (n = 76) were sensitive in both locomotion states. *Black lines* represent mean values for each subpopulation. Friedman test: *** = p < 0.001; ** = p < 0.005; * = p < 0.05; ns = p > 0.05. **B**, Tetrode tracks of the neurons shown in C. **C**, Circular plots of two neurons recorded from two butterflies [color code as in (B)] that changed their sensitivity after CDM application in quiescent animals. Corresponding spike shapes (*mean ± IQR*) and correlation coefficients (*corr*) are shown at the top left corner of each circular plot. **D**, Activity of 24 neurons (*Left*: tuning before application; *right*: tuning after application) that gained/lost angular sensitivity to the sun stimulus after CDM application. **E,** Comparison of vector strengths before (*pre*) and after CDM application. *Cyan* and *magenta* dots represent neurons that showed angular sensitivity exclusively after or before application. Neurons encoding the solar azimuth irrespective of CDM application are shown in *orange*. **F,** Statistical comparison of vector strengths before (*pre*) and after CDM application (Wilcoxon signed rank test: *** = p < 0.001; ** = p < 0.005). **G**, Preferred firing directions were stable after CDM application.

263 **Integration of idiothetic and visual inputs induces remapping during flight**

264 During steering flight, insects receive a multitude of different idiothetic signals, including
265 proprioceptive signals from flight muscles [29], vestibular-like signals [30], and motor efference copies.
266 Vestibular-like signals inform animals about rotations and provide sufficient information to encode the
267 insect's heading even when the animals orient in darkness [13,30]. To test the relevance of vestibular-like
268 signals for heading coding in monarch butterflies, we mounted the butterflies on a rotation stage in the
269 arena's center. This allowed us to rotate the butterflies by 360° in the presence of a static sun stimulus
270 (*quiescent rotation*; Fig. 6A and Supplementary Movie 6) followed by a rotation in darkness (*darkness*
271 *rotation*). Similar to results in cockroaches [30] and rodents [31,32], in these conditions, the preferred firing
272 directions of the butterfly neurons were invariant to the presence of visual stimuli (Fig. 6B-E; n = 16
273 neurons; V-test: $p < 0.0001$). The persistence of the neural tuning in darkness shows that the neurons
274 represented heading directions in quiescence. The neural tuning during *darkness rotation* was broader
275 than during *quiescent rotation* (Wilcoxon signed rank test: $p = 0.0076$; Fig. 6D and Supplementary
276 Figure 4), consistent with the fact that computing heading directions only with idiothetic cues
277 accumulates errors over time [10]. The preferred firing directions measured in the presence (*quiescent*
278 *rotation*) and absence (*quiescent*) of vestibular-like signals were almost identical (Fig. 6D and 6F; n =
279 16 neurons; V-test: $p < 0.0001$). Therefore, vestibular-like signals alone did not account for remapping
280 of the heading-direction network as observed in the same neurons during *steering flight* (Fig. 6D and
281 6G; n = 16 neurons; Rayleigh test: $p = 0.6$). Alternatively, steering commands in the form of motor
282 efference copies and reafference signals might trigger remapping. Each motor command is internally
283 stored and compared with reafferent signals, representing sensory feedback associated with turns [33-36].
284 This closed loop, from here on referred to as an "efference-reafferent loop", allows the animal to predict
285 sensory changes associated with turns. To test the influence of the "efference-reafferent loop" on
286 heading coding, we tethered the butterflies and suspended them to a rotation stage that allowed us to
287 subject them to 360° rotations and thus control their heading during fixed flights (Fig. 6H; *rotation fixed*
288 *flight*; Supplementary Movie 7). We found that even in the presence of vestibular-like and
289 proprioceptive signals in the absence of a functional "efference-reafferent loop", the heading-direction
290 network of butterflies performing fixed flights showed the same angular tuning as during *quiescence*

291 (Fig. 6I-6J; n = 17 neurons; V-test: $p < 0.001$). Thus, our results indicate that a proper "efference-
292 reafferent loop" is essential to transform the monarch butterfly heading-direction network into a
293 compass during steering flight.

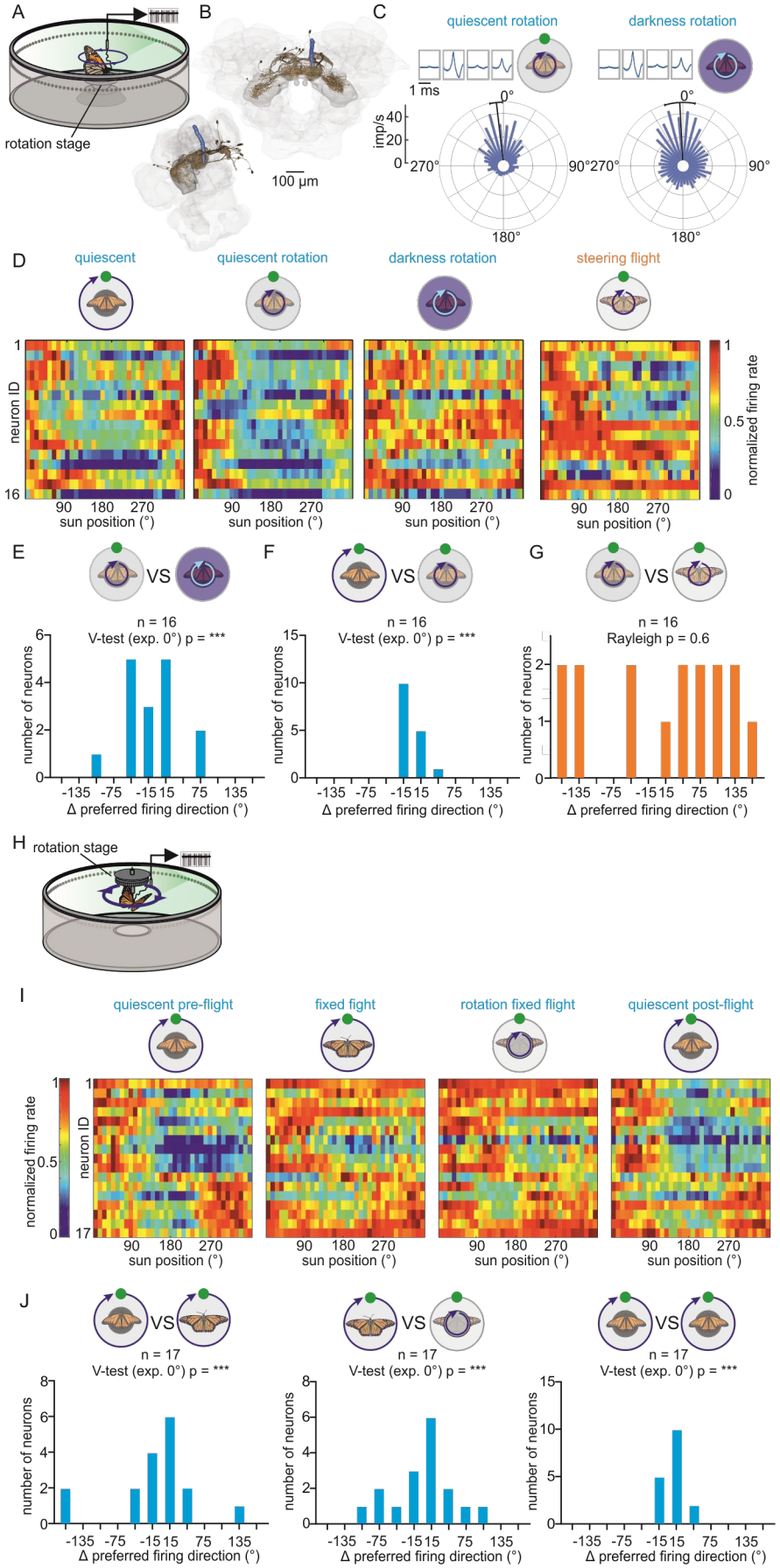

Fig. 6 | Motor efference copies and reafference signals induce remapping of the heading-direction network during flight. A, Illustration of the setup to test for the influence of vestibular-like signals. Angular sensitivity was measured while

rotating a quiescent butterfly on a rotation stage. **B**, Tetrode position during the experiment in which the example neuron in (C) was recorded. **C**, A neuron showing a preferred firing direction when the butterfly was rotated in the presence of the sun stimulus (*left*) and in darkness (*right*). **D**, Neural activity from 16 neurons in each behavioral state is plotted against the sun position. Only neurons that were sensitive (Rayleigh test: $p < 0.05$) in all behavioral states are included. **E-G**, Changes in the preferred firing direction during *quiescent rotation* and rotation in darkness (*darkness rotation*) (E); in the absence (*quiescent*) and in the presence of vestibular-like input (*quiescent rotation*) (F); and *quiescent rotation* and *steering flight* (G). **H**, Illustration of the setup to test for the influence of vestibular-like and proprioceptive signals. Angular sensitivity was measured while rotating a suspended tethered butterfly that was allowed to perform flight but not to steer (*rotation fixed flight*). **I**, Neural activity of 17 neurons for each behavioral state, i.e. quiescent pre-flight, fixed flight, rotation fixed flight, and quiescent post-flight is plotted against the sun position. **J**, Changes in preferred fight direction between quiescent pre-flight and fixed flight (*left*), quiescent pre-flight and rotation fixed flight (*middle*), and quiescent pre-flight and quiescent post-flight (*right*).

Idiothetic cues processed during steering flight dominate over visual cues

The explicit heading representation observed during flight in our "2-sun experiment" (Fig. 4) might be established by a hierarchy of cues during steering flight. To examine which sensory input, i.e. visual or idiothetic, is the most relevant for the heading-direction network in different behavioral states, we performed experiments in which both inputs were set in conflict in quiescent and steering flying butterflies. This was accomplished by displacing the sun stimulus by 180° during the experiment. When displacement occurred in quiescent rotating butterflies, the neural tuning shifted with the sun by about 180° (Fig. 7A-B; $n = 37$ neurons; V-test: $p < 0.001$). These results show that the coding of heading is dominated by the sun stimulus when quiescent animals are rotated when these receive vestibular-like inputs (see Fig. 6C-E). Interestingly, when we repeated the same experiments with steering flying butterflies, the neural tuning did not shift after stimulus displacement (Fig. 7C-D; $n = 22$ neurons; V-test: $p = 0.02$ with 0° as expected value). Thus, although the butterflies had the same stimulus setting during *quiescence* and *steering flight*, we demonstrate the existence of a state-dependent switch in the cue hierarchy in monarch butterflies. While the sun position dominated the heading coding in quiescence, idiothetic cues such as the "efference-reafferent loop" were ranked higher than the sun during flight.

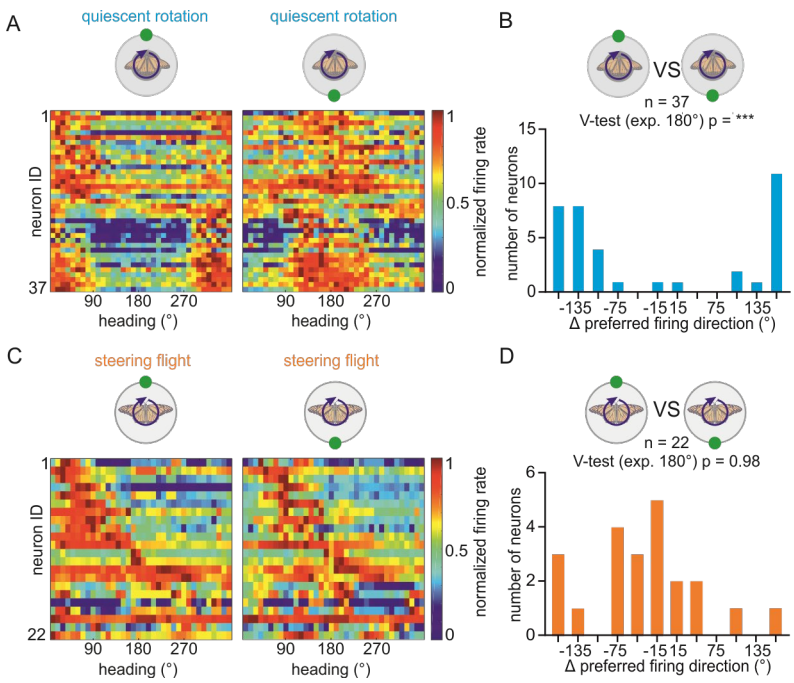

Fig. 7 | Heading coding is dominated by visual cues during quiescence while idiothetic cues dominate during flight. A, The neural activity of 37 neurons plotted against the animal's heading when the sun stimulus was positioned at 0° (*left*) and 180° (*right*) and the animal was rotated by 360° around its body axis (*rotation*). **B,** Changes in the preferred firing direction between the sun stimulus positioned at 0° and at 180° when the animal was rotated. Most neurons shifted their preferred firing directions by 180° (V-test: $p < 0.001$). **C,** The neural activity of 22 neurons plotted against the animal's heading when the sun stimulus was positioned at 0° (*left*) or at 180° (*right*) while the animals were able to steer during flight. **D,** The changes in preferred firing direction between the sun stimulus positioned at 0° and at 180°. The change of preferred firing direction was clustered around 0°.

Discussion

In the present study, we show substantial state-dependent effects in the heading-direction network of the monarch butterflies, including flight-induced octopaminergic changes in angular sensitivity and steering-induced changes in angular tuning. We provide the first evidence in insects that actual steering has a strong impact on the processing of heading information in the brain, as previously shown in mammals [31,37], and demonstrates the biological relevance of state-dependent changes in the central complex. Depending on the locomotory state, the heading-direction network switches from a sun-bearing coding in *quiescence* to a proper sun compass coding during flight. A compass tiling 360° of azimuth allows a robust representation of the butterfly' heading even under ambiguous (2-sun experiment) or variable (conflict experiment) visual settings. Robust heading representation is essential for migratory butterflies as they must maintain a stable flight course over an enormous distance while travelling through diverse visual scenes.

Changes in angular sensitivity of heading-direction neurons

While recent studies reported state-dependent sensitivity changes of central-complex neurons [22,23,38], the neural mechanisms underlying these changes have remained elusive. State-dependent changes in more peripheral brain regions like the optic lobes of blowflies [26] and *Drosophila* [39-41] have been attributed to a flight-induced increase in the octopamine levels. Our results suggest that octopamine contribute to flight-induced changes in angular sensitivity of central-complex neurons. Unlike what has been shown in visual neurons of fruit flies [41], changes in angular sensitivity did not correlate with a state-dependent change in the firing rate. In *Drosophila*, it has been reported that ring neurons sending visual information into the E-PG network alter their sensitivity to visual cues in a state-dependent manner [14,17], making this cell type a possible neuronal substrate for the state-dependent changes in angular sensitivity found in monarch butterflies. By modulating the visual input from the population of ring neurons in a state-dependent manner, the heading-direction network of monarch butterflies could gain coding flexibility, similar to what has been reported in *Drosophila* [14,15].

Heading coding in quiescence

364 Our methodological approach allowed us for the first time in any insect to discriminate between
365 the influence of different idiothetic inputs on the heading coding, i.e. vestibular-like, proprioceptive and
366 motor efferences coupled with reafferent signals. In addition to visual input from ring neurons, E-PG
367 cells receive idiothetic input in the form of angular movement from P-EN cells [20,21]. Since only 5% of
368 our recorded neurons conjunctively encoded flight turns and heading, it is highly unlikely that our results
369 originate from recordings of P-EN cells or neurons downstream of E-PG cells that themselves encode
370 angular movements [42]. Thus, E-PG cells represent the most plausible candidate recorded neurons in
371 which remapping occurs in our study.

372 When quiescent butterflies were confronted with an ambiguous 2-sun stimulus, the heading-
373 direction network was not able to unambiguously encode a particular heading. This is because visual
374 cues dominated the heading coding in this situation, as also observed in our cue conflict experiment.
375 Visual inputs are transmitted via the R2/4d ring neurons into the E-PG network [14,17]. As ring neurons'
376 receptive fields are biased towards the fronto-lateral visual field in monarch butterflies [43], and also in
377 fruit flies [17], the dominance of visual input is expected to bias the heading-direction network to the
378 frontal visual field, which is what we observed in quiescent monarch butterflies. However, comparable
379 to what has been found in cockroaches [30], the butterfly' heading is not purely based on visual
380 information. It also relies on vestibular-like idiothetic cues, such as mechanosensory inputs. As
381 previously shown in fruit flies [18], mechanosensory signals from the antennae may be integrated via
382 another set of ring neurons into the butterfly' heading network to enable the actual heading to be
383 sustained even in darkness. However, our conflict experiments demonstrate that in quiescent butterflies
384 vestibular-like inputs would be less relevant than visual information from the sun stimulus, as allowing
385 butterflies to fly while mechanically blocking their steering was not sufficient to induce a change in the
386 preferred firing directions. This indicates that proprioceptive information from the flight apparatus is
387 not responsible for changes in the neurons' preferred firing direction. Thus, even in a flying butterfly
388 deprived from turns, the sun stimulus, and thus the ring neurons activity, dominate the coding of heading
389 in the central complex. The coding of heading based on visual inputs – and in the absence of steering
390 commands – will therefore manifest in a body-related sun-bearing coding in quiescence and during fixed
391 flight.

392

393 **Flight steering-dependent transformation into a sun compass**

394 When the tethered flying butterflies were free to steer, we observed substantial shifts in the
395 neurons' preferred firing directions extending the heading-direction network to a 360° representation of
396 angular space. Notably, the steering-induced switch to a 360° sun compass leads to an unambiguous
397 heading coding during flight even when animals oriented with an ambiguous 2-sun stimulus. This
398 requires the heading-direction network to relate the angular position of multiple cues with respect to the
399 animal's orientation, which results in an allocentric compass coding. We showed that this switch to a
400 compass coding depends on the integration of motor efference copies and reafferent signals into the
401 central complex. While the ring neurons dominate the coding in quiescence, our cue conflict experiment
402 suggests that the heading coding in E-PG cells is mainly controlled by idiothetic signals from P-EN
403 neurons during flight. The dominance of the P-EN input during flight was unexpected since results in
404 *Drosophila* demonstrated that the coding of heading is dominated by visual information [13,44], similar to
405 what has been found in vertebrates, including fish [9], birds [45], and rats [10]. The differences observed in
406 modality weighting in monarch butterflies could represent adaptations to a migratory lifestyle.
407 Anatomical differences between the heading-direction systems of *Drosophila* and migratory desert
408 locusts have been proposed to increase the robustness of the compass during long-distance navigation
409 [46]. Consistent with this idea, our results show that heading representation remains robust to sudden
410 changes in the solar azimuth. Under these conditions, the heading-direction network primarily relies on
411 idiothetic cues. The difference in modality weighting we observed in butterflies compared to previously
412 reported in *Drosophila* may also be of a methodological nature. In *Drosophila*, the heading-direction
413 network has been studied in head-fixed preparations with the visual stimulus moved according to
414 intended angular movements [13-15,18]. In our experiments, the monarch butterflies were actually steering
415 which results in more naturalistic idiothetic inputs, including motor efference copies, reafferent signals,
416 and vestibular-like signals than in head-fixed preparations.

417 Taken together, the transition of the heading-direction network into a sun-compass during flight requires
418 the integration of multimodal information into the central complex. In nature, additional inputs, such as
419 the time-compensation of the sun position [4,47,48] and/or the earth's magnetic field [49,50], may provide

420 additional cues to form a robust compass system that monarch butterflies use to efficiently maintain
421 proper course orientation during their long migratory journey.
422
423 **Online Methods**
424 **Animals**
425 Monarch butterflies (*Danaus plexippus*) were ordered as pupae from Costa Rica Entomology Supply
426 (butterflyfarm.co.cr) and kept in an incubator (HPP 110 and HPP 749, Memmert GmbH + Co. KG,
427 Schwabach, Germany) at 25°C, 80% relative humidity and 12:12 light/dark-cycle conditions. After
428 eclosion, the adult butterflies were transferred into a different incubator (I-30VL, Percival Scientific,
429 Perry, IA, USA) at 25°C and 12:12 light/dark condition. Adults had access to 15% sucrose diluted in
430 water *ad libitum*. In total, we tested 89 butterflies.
431
432 **Setup for simultaneous behavioral and electrophysiological recordings**
433 To record neural activity in the butterfly brain, signals from custom-built tetrodes (see Tetrodes and
434 Implantation) were passed through an electrode interface board (EIB-18; Neuralynx Inc., Bozeman, MT,
435 USA) and an adapter board (ADPT-DUAL-HS-DRS; Neuralynx Inc., Bozeman, MT, USA) to a
436 Neuralynx recording system (DL 4SX 32ch System, Neuralynx Inc., Bozeman, MT, USA). The neural
437 activity was monitored using the software Cheetah (Neuralynx Inc., Bozeman, MT, USA). During
438 recording, the heading direction of a butterfly was observed in a flight arena similar to the ones described
439 before [4,51]. The arena had an inner diameter of 32 cm and a height of 12 cm (Fig. 1A). A tungsten rod
440 was attached to the butterfly's thorax using a magnet (diameter = 3 mm; magnetic force = 4 N;
441 Supermagnete, Webcraft GmbH, Gottmadingen, Germany) as well as dental wax (Article: 54895
442 Omnident, Rodgau Nieder-Roden, Germany) and was connected dorsally to an optical encoder (E4T
443 miniature Optical Kit Encoder, US Digital, Vancouver, WA, USA) at the center of the arena. To avoid
444 wrapping the tetrode wires around the tungsten rod, the animals' rotatory movements were restricted to
445 358°. The heading direction was measured at a sampling rate of 100 Hz and with an angular resolution
446 of 3°. These measurements were then digitized (USB4 Encoder Data Acquisition USB Device, US
447 Digital, Vancouver, WA, USA). The animal's heading was observed in the US Digital software (USB1,

USB4: US Digital, Vancouver, WA, USA). A trigger signal at the onset of the behavioral recording was sent via an ATLAS analog isolator (Neuralynx Inc., Bozeman, MT, USA) and the adapter board to the Neuralynx recording system. This allowed us to align the behavioral data from the encoder with our neural recordings in the software Spike2 (version 9.0 Cambridge Electronic Devices, Cambridge, UK) after an experiment. The upper inner circumference of the flight arena was equipped with 144 RGB-LEDs (Adafruit NeoPixel, Adafruit Industries, New York, New York, USA) at an elevation of ~ 30° relative to the butterfly. One of these LEDs, when lit, provided a single green light spot as a stimulus (1.74×10^{13} photons/cm^2/s and 1.2° angular subtense, as measured at the center of the arena). Insects interpret such a stimulus as the sun [52-54]. The angular position of the green light spot was controlled with an Arduino MEGA 2560. An analog output from the Arduino was sent via the ATLAS analog isolator to the Neuralynx recording system and allowed us to align the stimulus presentation with the neural activity.

Tetrodes and Implantation

To record neural activity in the butterfly brain, we adopted and modified the recording method that has been successfully established in honeybees to record learning related plasticity [55-57]. A tetrode was built by waxing five (four recording wires and one differential wire) 18 cm long and 12.5 µm thin (10µm + insulation) copper wires (P155, Elektrisola, Reichshof-Eckenhagen, Germany) together. The tetrode was carefully threaded through two Pebax® tubes (each 2-4 cm in length; 0.026' inner diameter; Zeus Inc, Orangeburg, SC, USA) that served as attaching points to mount the tetrode to a glass capillary. Tetrode and glass capillary were then attached to an electrode holder (M3301EH; WPI, Sarasota, FL, USA). The tetrode wires were connected to different channels of the EIB-18. A separate wire was connected to the grounding pin of the EIB-18 and served as grounding wire. To reduce the resistance of each electrode to about 0.1-1 MΩ, the tips of the tetrode wires were plated with gold (Elektrolyt Gold solution, Conrad Electronic SE, Hirschau, Germany). The resistance of each tetrode wire was measured using a nanoZ (Multi Channel Systems MCS GmbH, Reutlingen, Germany). To position the tetrode in the butterfly brain, the electrode holder (together with the EIB-18 and the tetrode) was connected to a micromanipulator (Sensapex, Oulu, Finland). For tetrode implantation, a monarch butterfly was

476 horizontally restrained on a magnetic holder. The head was waxed to the thorax to avoid head
477 movements during recording and flight. The head capsule was opened dorsally and fat and trachea on
478 top of the brain were removed. To gain access to the central complex, the neural sheath on the dorsal
479 brain surface was carefully removed using fine tweezers. The grounding wire was placed posteriorly in
480 the head capsule. To identify the tetrode position, the tip of the tetrode was immersed in ALEXA 647
481 Hydrazide (A20502, Thermo Fisher Scientific GmbH, Dreieich, Germany) or ALEXA 568 Hydrazide
482 (A10437, Thermo Fisher Scientific GmbH, Dreieich, Germany) diluted in 0.5 M KCl. Tetrodes were
483 then inserted into the central brain while measuring neural signals with a sampling frequency of 30 kHz
484 and a band-pass filter (600-6000Hz). One of the five tetrode wires was selected as a reference in the
485 recording software and its signal was subtracted from the signals of the remaining four tetrode wires to
486 obtain a differential signal. After finding neurons encoding the angular position of the sun stimulus, the
487 tetrode and the grounding wire were held in place by adding a two-component silicone elastomer (Kwik-
488 Sil, WPI, Sarasota, FL, USA). After the Kwik-Sil hardened (~ 1 hour), the butterfly was carefully
489 unrestrained and connected to the end of the tungsten rod that was connected to the optical encoder. The
490 tetrodes were carefully removed from the glass capillary and attached to a Pebax® tube to the tungsten
491 rod. This setup allowed us to obtain stable neural recordings for several hours when the butterfly was
492 either tethered flying or quiescent on a platform.
493
494 **Visualization of electrode tracks**
495 After neural recording, the brain was dissected out of the head and fixated overnight in 4% formaldehyde
496 at 4°C. After fixation, the brain was transferred into sodium-phosphate buffer (NaPi) and rinsed for 2 x
497 20 and 3 x 20 minutes in 0.1 M phosphate buffered saline (PBS) and PBS with 0.3% Triton-X (PBT),
498 respectively. The brain was dehydrated with an ascending ethanol series (30% - 100%, 15 minutes each)
499 and immersed with a 1:1 ethanol-methyl-salicylate solution for 15 minutes, followed by a clearing step
500 in methyl-salicylate for at least 1 hour. The brain was embedded in Permount (Fisher Scientific GmbH,
501 Schwerte, Germany) between two cover slips and scanned with a confocal microscope (Leica TCS SP2,
502 Wetzlar, Germany) using a 10 x water immersion objective (HCX PL-Apo 10x/0.4 CS, Leica, Wetzlar,
503 Germany). To visualize the position of the tetrode, we reconstructed the tetrode tracks together with

504 subneurons of the central complex in 3D using the software Amira 5.3.3 (ThermoFisher, Germany). To
505 visualize the tetrode positions from different experiments, we afterwards registered the tetrode position
506 into the monarch butterfly standard central complex [7]. We used an affine (12-degrees of freedom),
507 followed by an elastic registration to transfer the neuropils of the individual central complexes into the
508 corresponding neuropils of the standard central complex. The registration and deformation parameters
509 were then applied to the tetrode reconstruction to visualize the tetrodes in one frame of reference.
510

511 **Spike sorting and spike shape analysis**

512 Recordings were spike sorted with the tetrode configuration implemented in Spike2 (version 9.00,
513 Cambridge Electronic Devices, Cambridge, UK). We used four spike detection thresholds (two upper
514 and two lower thresholds). The highest and lowest thresholds were set to avoid large voltage deflections
515 deriving from movement artifacts being misinterpreted as spikes. The time window for template
516 detection was set to 1.6 ms. After spike-sorting, a principal component analysis (PCA) was used to
517 evaluate and to redefine spike clusters, if necessary. Spike2 channels were exported as down-sampled
518 Matlab files (3 kHz) and the remaining analysis was done with custom written scripts in MATLAB
519 (Version R2019b, MathWorks, Natick, MA, USA). To analyze the spike shapes and to perform
520 correlation analysis, the WaveMark channels containing the spike-waveforms were additionally
521 exported as non-down-sampled Matlab files (30 kHz). To ensure that we recorded from the same neuron
522 throughout the experiment, we compared the neuron-specific spike shapes across different recording
523 periods. For each behavioral state e.g., *quiescent pre-flight, fixed flight, steering flight, quiescent post-*
524 *flight*, the average spike shape was constructed by calculating and merging the mean spike shape from
525 each recording electrode along the time axis. This resulted in a total time window of 6.4 ms (4 x 1.6 ms)
526 or 232 points corresponding to a sampling rate of 30 kHz for each behavioral state. The average spike
527 shape during pre-flight was compared to the average spike shapes measured during flight (e.g., *fixed*
528 *flight*, *steering flight*), and after flight (*quiescent post-flight*). This resulted in at least two correlation
529 coefficients per neuron. We used the lowest correlation coefficient of each neuron to compare it to a
530 modelled distribution of correlation coefficients generated by the correlation between the neuron's spike
531 shape during pre-flight and all spike shapes obtained within one set of experiments (150 neurons for the

532 state-dependent change experiments (Fig. 1,2,3,S2,S3); 55 neurons for pharmacological experiments
533 (Fig. 5); 47 neurons for the passive rotation experiments (Fig. 6,S4); 37 neurons for the experiment using
534 two suns (Fig 4)). The correlation with a randomly selected spike shape was repeated in total 1,000,000
535 times to obtain the distribution of correlation coefficients for each neuron. Only neurons that exhibited
536 a statistically higher neuron-specific correlation coefficient than the modelled correlation coefficients
537 ($p < 0.05$) were used for further analysis. 289 neurons passed this criterion and had an average
538 correlation coefficient of 0.94 ± 0.08 (mean ± SD).
539
540 **Experiment testing state-dependent changes in the preferred firing direction**
541 To examine the neural response to a green light spot during quiescence, a green light spot was moved
542 360° around the animal during recording while the butterfly was sitting on a platform (Compact Lab
543 Jack, Inc, Newton, New Jersey, USA; *quiescent pre-flight*). The angular velocity of the sun stimulus
544 was set to 60°/s which is commonly used to characterize compass neurons in restrained insects [6,43,52].
545 The light spot was moved in clockwise and counterclockwise directions. While recording from the same
546 neuron, the stimulus condition was repeated (360° movement of the sun stimulus around the butterfly)
547 but this time while the animal performed a tethered flight in one locked direction (0°, the same heading
548 direction as in quiescence, *fixed flight*). Afterwards, the position of the sun stimulus remained stationary
549 at 0° while the tethered flying butterfly was free to rotate around its yaw axis (*steering flight*). In some
550 experiments (n = 63 neurons), the butterfly was allowed to sit on the platform again to measure the
551 neural response after flight (*quiescent post-flight*). To generate circular plots (bin size = 10°) showing
552 the spatial tuning of recorded neurons and to calculate the preferred firing directions and vector strengths
553 of each neuron, the CircStat [58] and CircHist [59] toolboxes of MATLAB were used. The neural sensitivity
554 for coding the angular position of the sun stimulus was examined by testing if the neural response
555 showed a non-uniform distribution ($p < 0.05$, Rayleigh test). If this was the case in one of the conditions,
556 the preferred firing direction and the vector strength of a neuron was calculated.
557
558 **Pharmacological experiments**

559 For the pharmacological experiments, we did not fix the tetrode's position with Kwik-Sil to ensure that
560 we still had access to the brain during the entire experiment.
561 For the pharmacological experiments, 10-20 µL of 500 µM chlordimeform (an octopamine agonist)
562 diluted in saline was topically applied onto the brain while performing neural recordings in quiescent
563 animals. We decided for a relatively high concentration of chlordimeform because the body dimensions
564 of the monarch butterfly are larger than that of flies [26,28] and we had to ensure that enough chlordimeform
565 diffused to the central complex (depth: 200-300µm). The neural sensitivity for coding the angular
566 position of the light spot was measured before treatment and in 10-minute intervals from the onset of
567 chlordimeform treatment. The stimulus was moved around the animal in the same way as described
568 above for quiescence. The neurons were recorded for about 40-140 minutes (mean = 70 ± 29 minutes).
569 The neural sensitivity to the stimulus was measured before treatment and compared with the last
570 measurement.
571
572 **The influence of stimulus history and velocity on neural tuning**
573 To test for the influence of stimulus history on neural tuning, the simulated sun was moved with a
574 constant velocity of 60°/s in an unpredictable manner around a quiescent butterfly (*unpredictable*
575 *stimulus history*). To test for changes in preferred firing directions associated with stimulus velocity, we
576 also varied the velocity of the sun stimulus between 20-80°/s while it was moved in an unpredictable
577 manner around the animal (*unpredictable stimulus velocity*; stimulus details are plotted in Fig. S3A).
578 The preferred firing directions obtained in these experiments were compared to the neural response of a
579 predictable moving sun stimulus (*quiescent*). At the end of each experiment, the preferred firing
580 directions were also measured during flight (*steering flight*). The preferred firing directions in
581 *quiescence* and during *steering flight* were compared with the preferred firing directions obtained in
582 response to the unpredictably moving sun stimulus conditions (n = 42 neurons). A V-test (expected
583 mean: 0°) was used to test if the change in preferred firing direction was similar between two conditions.
584 If the V-test was significant ($p < 0.05$) this means that data were clustered around 0° implying that the
585 preferred firing direction did not change between the tested conditions.
586

587 **Testing for coding of turning behavior**

588 To test whether the recorded central-complex neurons encoded flight turns, we selected the flight
589 sections in which the animal's heading changed more than 9° from its actual heading direction. We set
590 9° as threshold for turns because the angular sensitivity of the optical encoder was 3° and deviations of
591 ± 3° could represent variations in flight direction rather representing flight turns. We then examined the
592 firing rate prior to and after the moment of a turn during a one-second window (500 ms prior and 500
593 ms after a flight turn). The neural activity during the turn was normalized to the firing rate 500 ms prior
594 to the turn and was compared to the firing rate of sections in which the animal flew straight. Neurons
595 were categorized as coding for flight turns if (i) changes in the normalized neural activity during flight
596 turns were higher/lower than the changes occurring during periods of no turns (Wilcoxon p-test < 0.05)
597 or (ii) if changes in the normalized neural activity during time windows of flight turns fitted a Gaussian
598 distribution (> 0.6). 12 of the 150 (8%) neurons passed both criteria and were defined as neurons coding
599 for flight turns. Only 7 of these 12 neurons additionally encoded the angular position of the light spot
600 during flight.

601

602 **Passive rotation experiments**

603 To test for the influence of idiothetic cues on neural tuning, we mounted a platform on a rotation stage
604 (DT-50, PI miCos, Eschbach, Germany) at the center of the LED arena. The butterfly was then fixed on
605 the platform and the animal was rotated around its yaw axis. The motions of the rotation stage were
606 controlled by a custom written script in MATLAB. The neural response was first measured during
607 *quiescence* as described above. Then, the butterfly was rotated clockwise and counterclockwise at 60°/s
608 (*quiescence rotation*). During *quiescence rotation*, the sun stimulus was presented at 0° (in front of the
609 animal at the beginning of rotation). Afterwards, the butterfly was rotated in the same way, but in the
610 absence of any visual cue (*darkness rotation*). At the end of the experiment, the butterfly was
611 unrestrained, and the neural response was measured while the butterfly was allowed to fly (*steering*
612 *flight*). The directedness of the neural response during *rotation* and *darkness rotation* was represented
613 by calculating the vector strength of the neural response. The preferred firing direction of each neuron
614 (n = 16) was calculated for each behavioral state (*rotation, darkness rotation*, *quiescence*, *steering*

615 *flight*). Only neurons that encoded the angular position of the simulated sun in all conditions were
616 considered. If the preferred firing directions were similar across conditions, then the changes in preferred
617 firing directions would cluster around 0° (V-test). Alternatively, if the changes were not found to cluster
618 around 0°, they were tested for a uniform distribution (Rayleigh test: $p > 0.05$).
619
620 To test how the neural tuning changes if the animal is engaged in flight but is passively turned (instead
621 of performing controlled steering), we performed similar experiments with the rotation stage mounted
622 above the tethered animal. The tethered animal was then connected to the rotation stage and was
623 passively rotated around its yaw axis (*rotation fixed flight*) while experiencing the simulated sun at 0°.
624 The neural response of the neurons was compared to the responses recorded during quiescent situation
625 (*quiescent pre-flight*) and when the animal was allowed to fly in one heading direction (*fixed flight*)
626 while the sun stimulus was moved around the animal (at a velocity of 60°/s). After flight, the neural
627 response was remeasured during quiescence (*quiescent post-flight*). The preferred firing directions of
628 17 neurons that encoded the angular position of the sun stimulus in all behavioral states were calculated
629 and compared with the preferred firing direction during *quiescence* (pre-flight).
630
631 **Conflict experiments**
632 To test the relevance of the sun-stimulus in different behavioral states, we performed the same
633 experiments as described above (*rotation*, *steering flight*), with the exception that the position of the sun
634 stimulus was switched to the opposite side of the arena (180°) after three clockwise and
635 counterclockwise rotations (*rotation*) or after 2 minutes of flight (*steering flight*). Afterwards, the
636 experiment was repeated with the sun stimulus located at 180° relative to its original position. The
637 change of the preferred firing direction was compared between the two conditions. If the preferred firing
638 direction changed by 180° (V-test, expected direction:180°), then the preferred firing directions were
639 dominated by the change in the simulated sun's position.
640 **Experiments with the two-sun stimulus**
641 For the experiments with the two suns, two equally bright (1.74×10^{13} photons/cm^2/s) green light spots
642 were positioned 180° apart from each other (at 0° and 180° with respect to the initial orientation of the

animal). The neural response was measured during *quiescence* (pre- and post-flight) while the two suns were moved clockwise and counterclockwise around the animal (angular velocity: 60°/s). Additionally, the neural response was measured while the tethered flying butterfly was able to steer in the presence of the two sun stimuli (*steering flight*). A weighted fit model was used to test if the neural response was described by a Gaussian (weight < 0.5; unimodal) or a sine-square function (weight > 0.5; bimodal) [52]. 33 central-complex neurons were sensitive in each of the three tested conditions (*quiescent pre-flight, steering flight, quiescent post-flight*). The weights were statistically compared across the conditions according to a RM one-way ANOVA + Holm Sidák's multiple comparison test (GraphPad Prism 9, GraphPad Software, San Diego, CA, USA).

Data and codes

Matlab files with the calculated response parameters of the neurons together with the Matlab-scripts used for the analysis and Arduino scripts used for stimulus presentation are accessible from the Figshare Repository: https://....

Acknowledgements We thank Marie Dacke, Keram Pfeiffer, and Jan Ache for their helpful comments on our manuscript and Jan Ache for providing us with chlordimeform for pharmacological experiments. We thank Vivek Jayaraman, Manu Madhav and Flavio Rocces for discussing our results. We thank Keram Pfeiffer and Konrad Öchsner for their help in setting up the LED stimulus and Fabian Schmalz for introducing Neuralynx and spike sorting in *spike2*. In addition, we thank Sergio Siles (butterflyfarm.co.cr) and Marie Gerlinde Blaese for providing us with monarch butterfly pupae.

Competing interests The authors declare no competing financial interests.

Funding This work was funded by the Emmy Noether program of the German Research Foundation granted to BeJ (Grant number: EL784/1-1) and a European Research Council Advanced Grant to EJW (MagneticMoth 741298).

1 Mouritsen, H. Long-distance navigation and magnetoreception in migratory animals. *Nature* **558**, 50-59, doi:10.1038/s41586-018-0176-1 (2018).
2 Reppert, S. M., Gegear, R. J. & Merlin, C. Navigational mechanisms of migrating monarch butterflies. *Trends Neurosci* **33**, 399-406, doi:10.1016/j.tins.2010.04.004 (2010).
3 Reppert, S. M., Guerra, P. A. & Merlin, C. Neurobiology of Monarch Butterfly Migration. *Annu Rev Entomol* **61**, 25-42, doi:10.1146/annurev-ento-010814-020855 (2016).
4 Mouritsen, H. & Frost, B. J. Virtual migration in tethered flying monarch butterflies reveals their orientation mechanisms. *Proc Natl Acad Sci U S A* **99**, 10162-10166, doi:10.1073/pnas.152137299 (2002).
5 Perez, S. M., Taylor, O. R. & Jander, R. A Sun compass in monarch butterflies. *Nature* **387**, 29-29, doi:DOI 10.1038/387029a0 (1997).
6 Heinze, S. & Reppert, S. M. Sun Compass Integration of Skylight Cues in Migratory Monarch Butterflies. *Neuron* **69**, 345-358, doi:10.1016/j.neuron.2010.12.025 (2011).
7 Heinze, S., Florman, J., Asokaraj, S., El Jundi, B. & Reppert, S. M. Anatomical basis of sun compass navigation II: the neuronal composition of the central complex of the monarch butterfly. *J Comp Neurol* **521**, 267-298, doi:10.1002/cne.23214 (2013).
8 Finkelstein, A. *et al.* Three-dimensional head-direction coding in the bat brain. *Nature* **517**, 159-164, doi:10.1038/nature14031 (2015).
9 Vinepinsky, E. *et al.* Representation of edges, head direction, and swimming kinematics in the brain of freely-navigating fish. *Sci Rep* **10**, 14762, doi:10.1038/s41598-020-71217-1 (2020).
10 Taube, J. S. The head direction signal: origins and sensory-motor integration. *Annu Rev Neurosci* **30**, 181-207, doi:10.1146/annurev.neuro.29.051605.112854 (2007).
11 Taube, J. S., Muller, R. U. & Ranck, J. B., Jr. Head-direction cells recorded from the postsubiculum in freely moving rats. I. Description and quantitative analysis. *J Neurosci* **10**, 420-435 (1990).
12 Cullen, K. E. & Taube, J. S. Our sense of direction: progress, controversies and challenges. *Nat Neurosci* **20**, 1465-1473, doi:10.1038/nn.4658 (2017).
13 Seelig, J. D. & Jayaraman, V. Neural dynamics for landmark orientation and angular path integration. *Nature* **521**, 186-+, doi:10.1038/nature14446 (2015).
14 Fisher, Y. E., Lu, J., D'Alessandro, I. & Wilson, R. I. Sensorimotor experience remaps visual input to a heading-direction network. *Nature* **576**, 121-125, doi:10.1038/s41586-019-1772-4 (2019).
15 Kim, S. S., Hermundstad, A. M., Romani, S., Abbott, L. F. & Jayaraman, V. Generation of stable heading representations in diverse visual scenes. *Nature* **576**, 126-131, doi:10.1038/s41586-019-1767-1 (2019).
16 Hulse, B. K. & Jayaraman, V. Mechanisms Underlying the Neural Computation of Head Direction. *Annu Rev Neurosci* **43**, 31-54, doi:10.1146/annurev-neuro-072116-031516 (2020).
17 Seelig, J. D. & Jayaraman, V. Feature detection and orientation tuning in the Drosophila central complex. *Nature* **503**, 262-266, doi:10.1038/nature12601 (2013).
18 Okubo, T. S., Patella, P., D'Alessandro, I. & Wilson, R. I. A Neural Network for Wind-Guided Compass Navigation. *Neuron* **107**, 924-940 e918, doi:10.1016/j.neuron.2020.06.022 (2020).
19 Hardcastle, B. *et al.* A visual pathway for skylight polarization processing in Drosophila. *Elife* **10**, doi:ARTN e63225

10.7554/eLife.63225 (2021).
20 Turner-Evans, D. *et al.* Angular velocity integration in a fly heading circuit. *Elife* **6**, doi:10.7554/eLife.23496 (2017).
21 Green, J. *et al.* A neural circuit architecture for angular integration in Drosophila. *Nature* **546**, 101-+, doi:10.1038/nature22343 (2017).
22 Weir, P. T. & Dickinson, M. H. Functional divisions for visual processing in the central brain of flying Drosophila. *Proc Natl Acad Sci U S A* **112**, E5523-5532, doi:10.1073/pnas.1514415112 (2015).

23 Rosner, R., Pegel, U. & Homberg, U. Responses of compass neurons in the locust brain to visual motion and leg motor activity. *J Exp Biol* **222**, doi:10.1242/jeb.196261 (2019).
24 Martin, J. P., Guo, P. Y., Mu, L. Y., Harley, C. M. & Ritzmann, R. E. Central-Complex Control of Movement in the Freely Walking Cockroach. *Current Biology* **25**, 2795-2803, doi:10.1016/j.cub.2015.09.044 (2015).
25 Orchard, I., Ramirez, J. M. & Lange, A. B. A Multifunctional Role for Octopamine in Locust Flight. *Annual Review of Entomology* **38**, 227-249, doi:DOI 10.1146/annurev.en.38.010193.001303 (1993).
26 Longden, K. D. & Krapp, H. G. State-Dependent Performance of Optic-Flow Processing Interneurons. *J Neurophysiol* **102**, 3606-3618, doi:10.1152/jn.00395.2009 (2009).
27 Ache, J. M., Namiki, S., Lee, A., Branson, K. & Card, G. M. State-dependent decoupling of sensory and motor circuits underlies behavioral flexibility in Drosophila. *Nature Neuroscience* **22**, 1132-+, doi:10.1038/s41593-019-0413-4 (2019).
28 Jung, S. N., Borst, A. & Haag, J. Flight activity alters velocity tuning of fly motion-sensitive neurons. *J Neurosci* **31**, 9231-9237, doi:10.1523/JNEUROSCI.1138-11.2011 (2011).
29 Kathman, N. D. & Fox, J. L. Representation of Haltere Oscillations and Integration with Visual Inputs in the Fly Central Complex. *Journal of Neuroscience* **39**, 4100-4112, doi:10.1523/Jneurosci.1707-18.2019 (2019).
30 Varga, A. G. & Ritzmann, R. E. Cellular Basis of Head Direction and Contextual Cues in the Insect Brain. *Curr Biol* **26**, 1816-1828, doi:10.1016/j.cub.2016.05.037 (2016).
31 Shinder, M. E. & Taube, J. S. Self-motion improves head direction cell tuning. *J Neurophysiol* **111**, 2479-2492, doi:10.1152/jn.00512.2013 (2014).
32 Coletta, S., Frey, M., Nasr, K., Preston-Ferrer, P. & Burgalossi, A. Testing the Efficacy of Single-Cell Stimulation in Biasing Presubicular Head Direction Activity. *Journal of Neuroscience* **38**, 3287-3302, doi:10.1523/Jneurosci.1814-17.2018 (2018).
33 von Holst, E. & Mittelstaedt, H. Das Reafferenzprinzip - (Wechselwirkungen Zwischen Zentralnervensystem Und Peripherie). *Naturwissenschaften* **37**, 464-476, doi:Doi 10.1007/Bf00622503 (1950).
34 Heisenberg, M. & Wolf, R. On the Fine-Structure of Yaw Torque in Visual Flight Orientation of Drosophila-Melanogaster. *J Comp Physiol* **130**, 113-130, doi:Doi 10.1007/Bf00611046 (1979).
35 Webb, B. Neural mechanisms for prediction: do insects have forward models? *Trends Neurosci* **27**, 278-282, doi:10.1016/j.tins.2004.03.004 (2004).
36 Kim, A. J., Fitzgerald, J. K. & Maimon, G. Cellular evidence for efference copy in Drosophila visuomotor processing. *Nature Neuroscience* **18**, 1247-+, doi:10.1038/nn.4083 (2015).
37 Stackman, R. W., Golob, E. J., Bassett, J. P. & Taube, J. S. Passive transport disrupts directional path integration by rat head direction cells. *J Neurophysiol* **90**, 2862-2874, doi:10.1152/jn.00346.2003 (2003).
38 Bender, J. A., Pollack, A. J. & Ritzmann, R. E. Neural activity in the central complex of the insect brain is linked to locomotor changes. *Curr Biol* **20**, 921-926, doi:10.1016/j.cub.2010.03.054 (2010).
39 Suver, M. P., Mamiya, A. & Dickinson, M. H. Octopamine Neurons Mediate Flight-Induced Modulation of Visual Processing in Drosophila. *Current Biology* **22**, 2294-2302, doi:10.1016/j.cub.2012.10.034 (2012).
40 Maimon, G., Straw, A. D. & Dickinson, M. H. Active flight increases the gain of visual motion processing in Drosophila. *Nature Neuroscience* **13**, 393-U329, doi:10.1038/nn.2492 (2010).
41 Chiappe, M. E., Seelig, J. D., Reiser, M. B. & Jayaraman, V. Walking Modulates Speed Sensitivity in Drosophila Motion Vision. *Current Biology* **20**, 1470-1475, doi:10.1016/j.cub.2010.06.072 (2010).
42 Shiozaki, H. M., Ohta, K. & Kazama, H. A Multi-regional Network Encoding Heading and Steering Maneuvers in Drosophila. *Neuron* **106**, 126-+ (2020).

43 Nguyen, T. A. T., Beetz, M. J., Merlin, C. & El Jundi, B. Sun compass neurons are tuned to migratory orientation in monarch butterflies. *Proc Biol Sci* **288**, 20202988, doi:10.1098/rspb.2020.2988 (2021).
44 Kim, S. S., Rouault, H., Druckmann, S. & Jayaraman, V. Ring attractor dynamics in the Drosophila central brain. *Science* **356**, 849-U111, doi:10.1126/science.aal4835 (2017).
45 Ben-Yishay, E. *et al.* Directional tuning in the hippocampal formation of birds. *Curr Biol*, doi:10.1016/j.cub.2021.04.029 (2021).
46 Pisokas, I., Heinze, S. & Webb, B. The head direction circuit of two insect species. *Elife* **9**, doi:ARTN e53985

10.7554/eLife.53985 (2020).
47 Sauman, I. *et al.* Connecting the navigational clock to sun compass input in monarch butterfly brain. *Neuron* **46**, 457-467, doi:10.1016/j.neuron.2005.03.014 (2005).
48 Merlin, C., Gegear, R. J. & Reppert, S. M. Antennal Circadian Clocks Coordinate Sun Compass Orientation in Migratory Monarch Butterflies. *Science* **325**, 1700-1704, doi:10.1126/science.1176221 (2009).
49 Guerra, P. A., Gegear, R. J. & Reppert, S. M. A magnetic compass aids monarch butterfly migration. *Nat Commun* **5**, 4164, doi:10.1038/ncomms5164 (2014).
50 Wan, G., Hayden, A. N., Iiams, S. E. & Merlin, C. Cryptochrome 1 mediates light-dependent inclination magnetosensing in monarch butterflies. *Nat Commun* **12**, 771, doi:10.1038/s41467-021-21002-z (2021).
51 Franzke, M. *et al.* Spatial orientation based on multiple visual cues in non-migratory monarch butterflies. *J Exp Biol* **223**, doi:10.1242/jeb.223800 (2020).
52 el Jundi, B. *et al.* Neural coding underlying the cue preference for celestial orientation. *P Natl Acad Sci USA* **112**, 11395-11400, doi:10.1073/pnas.1501272112 (2015).
53 Edrich, W., Neumeyer, C. & Helversen, O. V. Anti-Sun Orientation of Bees with Regard to a Field of Ultraviolet-Light. *J Comp Physiol* **134**, 151-157, doi:Doi 10.1007/Bf00610473 (1979).
54 Rossel, S. & Wehner, R. Celestial Orientation in Bees - the Use of Spectral Cues. *J Comp Physiol* **155**, 605-613, doi:Doi 10.1007/Bf00610846 (1984).
55 Strube-Bloss, M. F., Nawrot, M. P. & Menzel, R. Mushroom body output neurons encode odor-reward associations. *J Neurosci* **31**, 3129-3140, doi:10.1523/JNEUROSCI.2583-10.2011 (2011).
56 Brill, M. F., Reuter, M., Rossler, W. & Strube-Bloss, M. F. Simultaneous long-term recordings at two neuronal processing stages in behaving honeybees. *J Vis Exp*, doi:10.3791/51750 (2014).
57 Strube-Bloss, M. F., Nawrot, M. P. & Menzel, R. Neural correlates of side-specific odour memory in mushroom body output neurons. *Proc Biol Sci* **283**, doi:10.1098/rspb.2016.1270 (2016).
58 Berens, P. CircStat: A MATLAB Toolbox for Circular Statistics. *J Stat Softw* **31**, 1-21, doi:DOI 10.18637/jss.v031.i10 (2009).
59 Zittrell, F., Pfeiffer, K. & Homberg, U. Matched-filter coding of sky polarization results in an internal sun compass in the brain of the desert locust. *Proc Natl Acad Sci U S A* **117**, 25810-25817, doi:10.1073/pnas.2005192117 (2020).